

Article

Open Access



Rational design of Ru/TiO₂/CNTs as cathode: promotion of cycling performance for aprotic lithium-oxygen battery

Lili Liu^{1,*}, Congcong Zhou¹, Weiwei Fang^{2,*}, Yuyang Hou³, Yuping Wu¹

¹School of Energy Science and Engineering, Nanjing Tech University, Nanjing 211816, Jiangsu, China.

²International Innovation Center for Forest Chemicals and Materials, College of Chemical Engineering, Nanjing Forestry University, Nanjing 210037, Jiangsu, China.

³CSIRO Mineral Resources, Clayton, VIC 3168, Australia.

***Correspondence to:** Prof. Lili Liu, School of Energy Science and Engineering, Nanjing Tech University, Nanjing 211816, Jiangsu, China. E-mail: liulili@njtech.edu.cn; Prof. Weiwei Fang, International Innovation Center for Forest Chemicals and Materials, College of Chemical Engineering, Nanjing Forestry University, 159 Longpan Road, Nanjing 210037, Jiangsu, China. E-mail: wwfang2020@njfu.edu.cn

How to cite this article: Liu L, Zhou C, Fang W, Hou Y, Wu Y. Rational design of Ru/TiO₂/CNTs as cathode: promotion of cycling performance for aprotic lithium-oxygen battery. *Energy Mater* 2023;3:300011.
<https://dx.doi.org/10.20517/energymater.2022.68>

Received: 24 Oct 2022 **First Decision:** 28 Nov 2022 **Revised:** 19 Jan 2023 **Accepted:** 13 Feb 2023 **Published:** 23 Mar 2023

Academic Editors: Md Mokhlesur Rahman, Jia-Qi Huang **Copy Editor:** Fangling Lan **Production Editor:** Fangling Lan

Abstract

Realizing long-life cycling is the biggest challenge in the research field of Li-O₂ batteries in the current stage. The main reasons for poor cycling performance are the sluggish Li₂O₂ formation and decomposition process, as well as the side reaction of carbon cathode. In order to accurately address the problems above, a TiO₂/CNTs cathode was rationally designed for long-life Li-O₂ batteries. The CNTs skeleton offers multiple three-dimensional channels for the rapid transportation of oxygen, Li⁺ and electrons. A thin-film and discontinuous layer of TiO₂ is coated on the CNTs surface to effectively inhibit the carbon corrosion but still could let mass transfer smoothly. Ultrafine Ru nanoparticles decorating the TiO₂/CNTs serve as efficient catalytic active sites. Benefiting from the unique structure design, Li-O₂ batteries with the cathode of TiO₂/CNTs achieve a cycling life of 110 with a fixed capacity of 500 mAh g⁻¹ at a current density of 100 mA g⁻¹. Our research generates new ideas for designing long-cycling Li-O₂ battery cathodes.

Keywords: Lithium-oxygen battery, rational design cathode, side reaction, Li₂O₂, cycling performance



© The Author(s) 2023. **Open Access** This article is licensed under a Creative Commons Attribution 4.0 International License (<https://creativecommons.org/licenses/by/4.0/>), which permits unrestricted use, sharing, adaptation, distribution and reproduction in any medium or format, for any purpose, even commercially, as long as you give appropriate credit to the original author(s) and the source, provide a link to the Creative Commons license, and indicate if changes were made.



INTRODUCTION

Li-ion batteries are approaching their theoretical limit in energy density, although they have truly changed the world by serving as either portable or large-scale energy storage system^[1]. Nonaqueous lithium-oxygen (Li-O₂) battery, an emerging next-generation energy storage system, shows an extremely high theoretical energy density that is almost several times that of state-of-the-art Li-ion batteries^[2]. The electrochemistry of a nonaqueous Li-O₂ battery is simply based on the reaction between oxygen and Li on a porous cathode^[3-6]. Nevertheless, such a simple reaction conceals quite complicated aspects which affect the final performance of a Li-O₂ battery. With a certain electrolyte, the cathode and its structure and type of catalyst largely govern the formation route and the structure and morphology of the Li₂O₂, which in turn influences the capacity, overpotential and lifespan of Li-O₂ batteries.

So far, two main types of Li₂O₂ formation route have been studied and the intrinsic relationships of their structure and the electrochemical behaviors have been widely accepted by researchers^[3,4,7-11]. The Li-O₂ battery with toroidal-structured Li₂O₂ usually delivers a high discharge capacity because of its large size, which of course leads to a large charge overpotential to decompose. Film-or shape-structured Li₂O₂ are rather easier to decompose during charging process, but the cathode surface will be fully passivated once such a thin film is formed and the discharge process will be terminated, leading to a low capacity. As we all expect, large discharge capacity and low charge overpotential is the ultimate goal of developing Li-O₂ battery, which implies that the ideal Li₂O₂ should have premium size, crystalline and in particular the cathode surface should still feature a porous structure after being generated^[9,12-14]. Therefore, a variety of strategies to regulate the Li₂O₂ formation have been proposed, including rational cathode design, surface engineering, multicomponent catalyst employment, and so on^[15-19]. With these measures in hand, in recent years, Li₂O₂ with different favorable morphologies have been discovered, which helped decrease the overpotential and enlarge the capacity to some extent. However, the cycling performance is still far from satisfactory and needs more attention^[15-17]. As we all know, carbon materials show their overwhelming advantage in serving cathode in Li-O₂ batteries due to their low price and excellent electron conductivity^[20,21], but carbon corrosion upon battery cycling is an unavoidable factor that leads to battery failure^[22-24]. Therefore, designing a cathode that could regulate favorable Li₂O₂ formation/ decomposition and meanwhile could retain the merit of carbon materials while avoiding the side reactions will be of high significance to building long-life Li-O₂ batteries^[25,26].

Herein in this work, a rational design of TiO₂/CNTs cathode is presented. A thin and loose TiO₂ layer partially coats the CNTs surface, followed by decorating ultrafine Ru nanoparticles on the TiO₂/CNTs. Several advantages can be revealed in this cathode design: (i) The CNTs skeleton offers multiple three-dimensional channels for the rapid transportation of oxygen, Li⁺ and electrons; (ii) The large surface area provides huge space for Li₂O₂ accommodation; (iii) The thin-loose TiO₂ layer effectively inhibits the carbon corrosion but still could let mass transfer; and (iv) The ultrafine Ru nanoparticles serves as catalytic active sites. Taking these four aspects above in consideration, a long-life Li-O₂ battery is constructed.

EXPERIMENTAL

Preparation of the catalyst

A certain amount of the commercial multiwall carbon nanotubes (MWCNTs) was firstly oxidized with a solution (200 mL) that contained 75 mL nitric acid (65%-68%) and purified water under vigorous stirring overnight to remove impurities. Then it was washed with deionized water and ethanol several times, followed by drying at 80 °C in air.

TiO₂/CNTs was achieved by the hydrolysis of the titanium butoxide on the surface of CNTs, and the method was modified by a previous report^[27]. Ru nanoparticles were then loaded on the TiO₂/CNTs via a modified aqueous reduction route^[28]. In detail, in a flask (250 mL), a certain amount of RuCl₃·3H₂O was dissolved in 100 mL aqueous solution and then 100 mg of TiO₂/CNTs was added to form a mixture. This mixture was stirred for 24 h at room temperature. Afterwards, 10 mL aqueous solution of NaBH₄ was added dropwise to the previous solution to keep the molar ratio at 3 by controlling the volume of NaBH₄ and the weight of RuCl₃·3H₂O. The Ru/TiO₂/CNTs black powder was generated after 1 h vigorous stirring. Then, the resulting solid product was washed with water and ethanol via centrifugation several times and finally dried in a vacuum oven at 80 °C overnight.

Physical characterizations

X-ray diffraction (XRD) (GBC mini materials analyser MMA) patterns were performed at a scan rate of 4° min⁻¹ and analysed with Traces™ software coupled with the Joint Committee on Powder Diffraction Standards (JCPDS) powder diffraction files. The morphological information of the samples was characterized by field emission scanning electron microscopy (FE-SEM, JEOL 7500) and transmission electron microscopy (TEM, JEOL ARM-200F). The XPS result was analysed using CasaXPS software, and all the data were calibrated by C 1s at 284.6 eV for graphite.

Li-O₂ battery measurements

For the fabrication of the cathode, catalyst (80 wt.%), Ketjen Black (KB10 wt.%), and poly(1,1,2,2-tetrafluoroethylene) (PTFE) (60% dispersion, 10 wt.%) were mixed in an isopropanol solution to get a homogeneous slurry, which was then coated on carbon paper. Afterwards, the electrodes were dried in a vacuum oven at 120 °C overnight. All the lithium-oxygen batteries were assembled in an Ar-filled glove box (Mbraun, Unilab, Germany) with both water and oxygen contents below 0.1 ppm. 2032-type coin cells with 9 air holes on the cathode cape were employed as Li-O₂ batteries. Apart from cathode, in a typical Li-O₂ battery, lithium metal acted as the counter electrode while 1 M LiCF₃SO₃ dissolved in tetraethylene glycol dimethyl ether (TEGDME) worked as electrolyte. All the assembled coin cells were stored in an O₂-purged homemade chamber which was connected to the battery tester (LAND CT 2001) for 2 h before each test. The galvanostatic discharge-charge tests were then conducted in the potential range of 2.0-4.5 V (vs. Li⁺/Li). The loading amount in each cathode was about 0.6~0.8 mg cm⁻².

Examination of the discharged and recharged electrodes was realized by disassembling the batteries in the glove box, followed by rinsing the cycled electrode with tetraethylene glycol dimethyl ether (TEGDME) and removing the solvent under vacuum. For ex-situ SEM and XPS measurements, the collected electrodes were put in a plastic package and laminated in the glove box before taking them out to the outside instruments.

RESULTS AND DISCUSSION

Structure and morphology analysis

The fabrication process of the Ru/TiO₂/CNTs cathode consisted of two steps [Figure 1]. TiO₂/CNTs was firstly prepared by the hydrolysis of the titanium butoxide on the surface of CNTs. Ultrafine Ru nanoparticles were then loaded on TiO₂/CNTs via an aqueous reduction reaction. The rational designed Ru/TiO₂/CNTs cathode was anticipated to effectively catalyze the reversible Li₂O₂ formation and decomposition.

The CNTs had a diameter of 15 nm and showed a very distinct layered structure of nano-walls [Figure 2A]. Both light and dart fields were utilized to well characterize the microstructure of Ru/CNTs and Ru/TiO₂/CNTs. Ultrafine Ru nanoparticles with a size of 2-3 nm were decorated on the surface of CNTs in the sample of Ru/CNTs [Figure 2B and C]. The existence of TiO₂ in the sample of Ru/TiO₂/CNTs

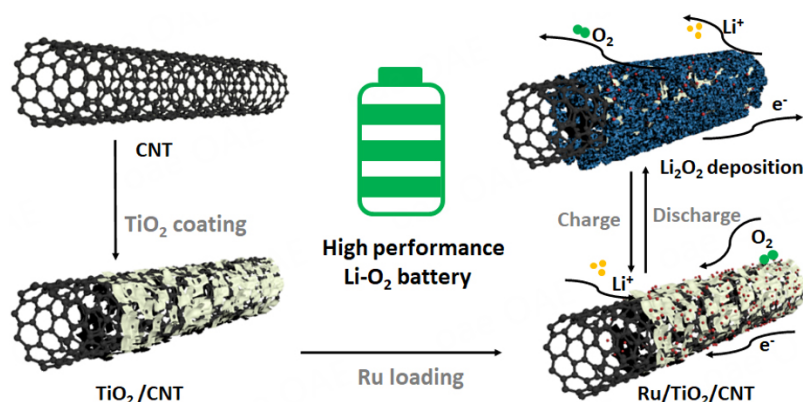


Figure 1. Schematic illustration of the preparation route of Ru/TiO₂/CNTs.

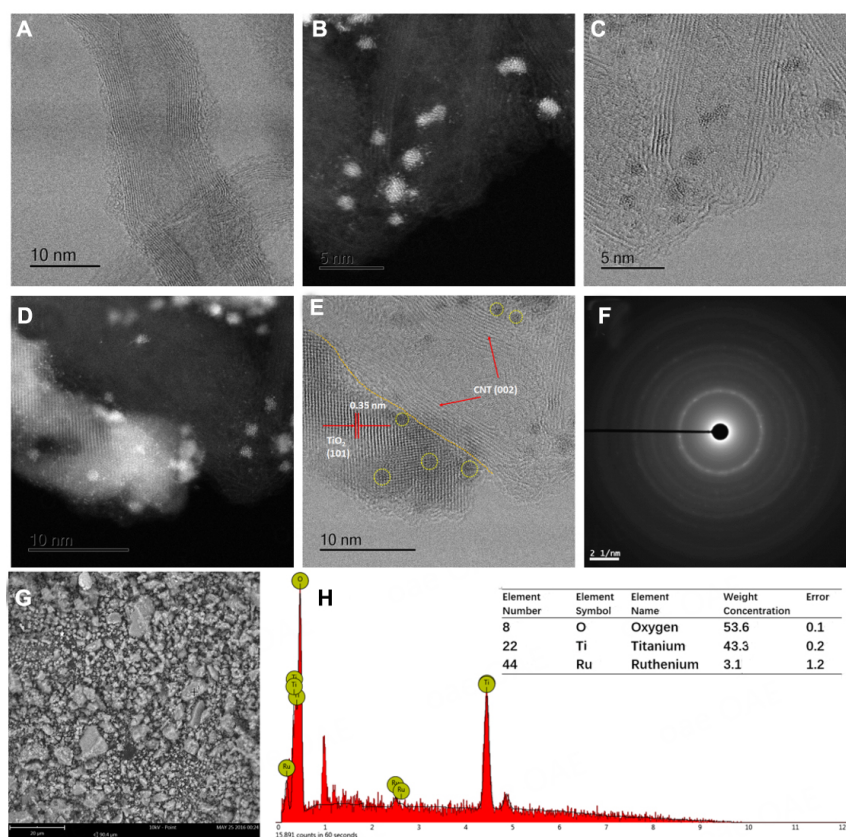


Figure 2. Physical characterizations. (A) TEM images of CNTs, HRTEM image of Ru/CNTs (B) dark field and (C) light field, HRTEM image of Ru/TiO₂/CNTs (D) dark field and (E) light field; (F) SAED pattern of Ru/TiO₂/CNTs; (G) SEM and (H) EDX of Ru/TiO₂/CNTs.

nanocomposites could be evidenced by the typical interplanar spacings of 0.35 nm, which was well consistent with the *d*-spacing of the (101) crystal planes of rutile TiO₂ (JCPDS 21-1272) [Figure 2D and E]. Meanwhile, Ru nanoparticles could also be found deposited on the surface of TiO₂, which could be further evidenced by HR-TEM element mapping [Supplementary Figure 1]. The indexed diffraction rings in the selected area electron diffraction (SAED) pattern also verified the rutile structure of TiO₂ [Figure 2F]. The EDX spectrum of the Ru/TiO₂/CNTs also verified the material constitution, and showed that the loading

amount of Ti and Ru was 3.1% and 43.3% (atom weight percentage) [Figure 2G and H]. The specific surface area of the Ru/TiO₂/CNTs is 968.3 m²/g.

The XRD pattern of CNTs showed typical broad diffraction peaks of the (002) and (100) planes of carbon, while TiO₂/CNTs delivered several diffraction peaks attributed to (101), (200), (211), (204), and (440) planes, which were assigned to rutile TiO₂ (JCPDS (21-1272) [Figure 3A]^[29,30]. Notably, no peak for Ru was found in the results of the Ru/TiO₂/CNTs due to its low content. X-ray photoelectron spectroscopy (XPS) of the Ru/TiO₂/CNTs confirmed the co-existence of Ru, Ti, O, and C elements [Figure 3B], and the binding energy of Ti 2p_{1/2} and Ru3p^{3/2} overlapped at approximately 465 eV. Four individual component peaks can be identified as C-C (284.6 eV), C-O (285.3 eV), C=O (287.5 eV), and O-C=O (288.5 eV), respectively [Figure 3C]^[25]. O 1s orbital BE spectra of the Ru/TiO₂/CNTs sample [Figure 3D] identified two peaks at 530.8, and 532.5 eV, indicating the O 1s binding energy of lattice oxygen (O1) and oxygen vacancy (O2), respectively^[14,31]. The peaks at 459.0 eV and 465.08 eV in the fine spectrum of Ti proved the successful formation of TiO₂ [Figure 3E]. The peaks for Ru 3p_{1/2} at 464.8 eV were assigned to the photoemission from (Ru⁰) and the peak at 465.8 eV was attributed to RuO₂ (Ru⁴⁺) [Figure 3F], which could be due to partial oxidation of Ru^[32-34].

Electrochemical performance analysis

The initial discharge-charge curves of cells with the three samples in the potential range of 2.0-4.5V (vs. Li/Li⁺) at a current density of 0.1 mA g⁻¹ were measured [Figure 4A]. Cells with Ru/CNTs and Ru/TiO₂/CNTs cathodes showed obviously smaller charge overpotential and larger capacities than those of CNTs, because of the high catalytic efficiency of Ru catalyst. Meanwhile, the capacity of Ru/TiO₂/CNTs was almost 1000 mAh g⁻¹ higher than that of Ru/CNTs. Both cathodes showed similar initial discharge-charge behavior at a fixed discharge depth. It is worth noting that the discharge overpotential of the Ru/TiO₂/CNTs was a bit larger than that without TiO₂ [Figure 4B]. We speculate that the low-conductive TiO₂ showed a weak effect on the Li₂O₂ nucleation during the first cycle. However, the discharge terminal potential recovered in the subsequent cycling process. Compared with the cell of Ru/CNTs [Figure 4C], the discharge and charge plots in fixed capacity kept quite stable [Figure 4D]. A rather clear comparison could be observed from the evolution process of the discharge terminal potential with a fixed capacity of 500 mAh g⁻¹. A cycle life of almost 110 was achieved when using the Ru/TiO₂/CNTs cathode [Figure 4E]. The prolonged lifespan could be approximately benefited from the thin TiO₂ layer that effectively inhibited carbon corrosion and electrolyte loss.

Discharge and charge mechanism analysis

To further explore how the as-prepared Ru/TiO₂/CNTs cathode worked on the mechanism of the Li-O₂ battery, the morphological evolution of the cathode was characterized by SEM at different cycling states. The fresh electrode showed a porous structure [Figure 5A]. Snow-like material appeared on the whole surface of the electrode after the first discharge [Figure 5B], but disappeared after recharge [Figure 5C]. The reversible formation and disappearance of the discharge product indicated that the Ru/TiO₂/CNTs cathode could probably catalyze the Li₂O₂ formation and decomposition. More importantly, unlike traditional toroidal-like or film-like discharge products, which either needed large charge overpotential to decompose or totally passivate the electrode surface, the as-prepared Ru/TiO₂/CNTs cathode still featured a porous state after discharge and the Li₂O₂ showed crystalline-like structure with premium size. Thus, the ORR and especially OER kinetics based on such structured-Li₂O₂ should be remarkably boosted and the above-mentioned electrochemical results powerfully verified this. The electrode surface became not as sharp as the fresh one after 30 cycles, but still porous [Figure 5D]. Agglomeration of porous particles appeared on the cathode when the cycle life reached 60 [Figure 5E], which was probably due to the gradual accumulation of the side product and the uncompleted decomposition of the discharge product. After another further 40

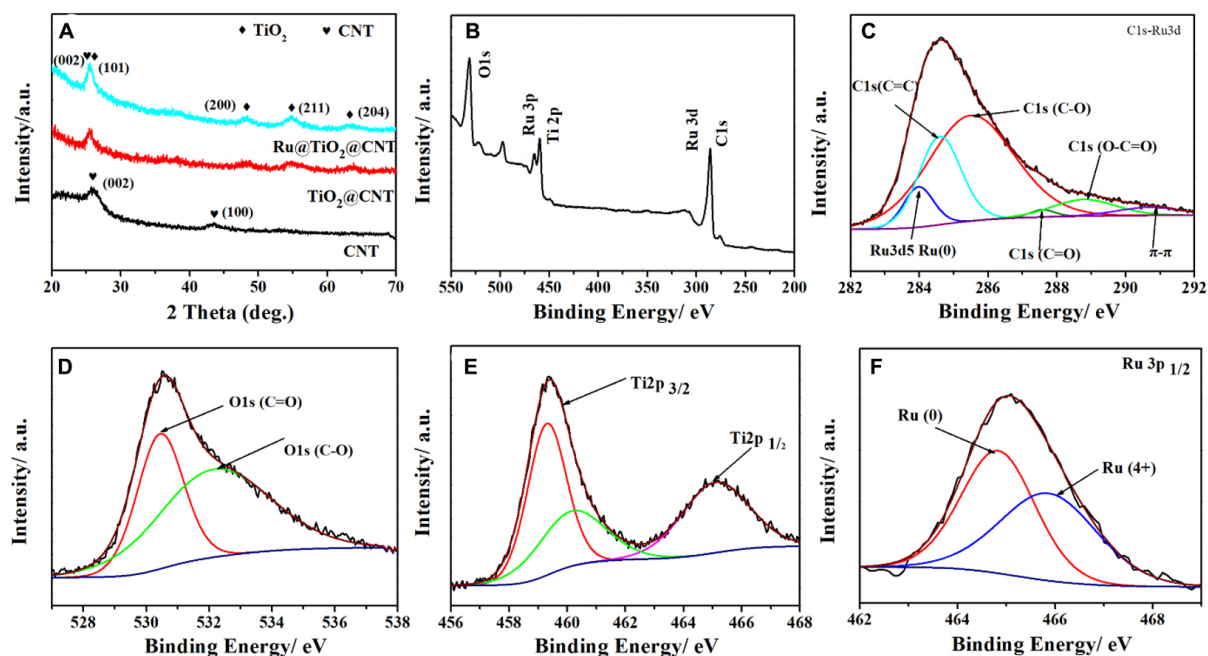


Figure 3. (A) XRD patterns of the pure CNTs, TiO₂/CNTs and Ru/TiO₂/CNTs samples; (B) XPS spectra of the Ru/TiO₂/CNTs; High-resolution XPS spectra for (C) C 1s; (D) O 1s; (E) Ti 2p and (F) Ru 3p of the Ru/TiO₂/CNTs.

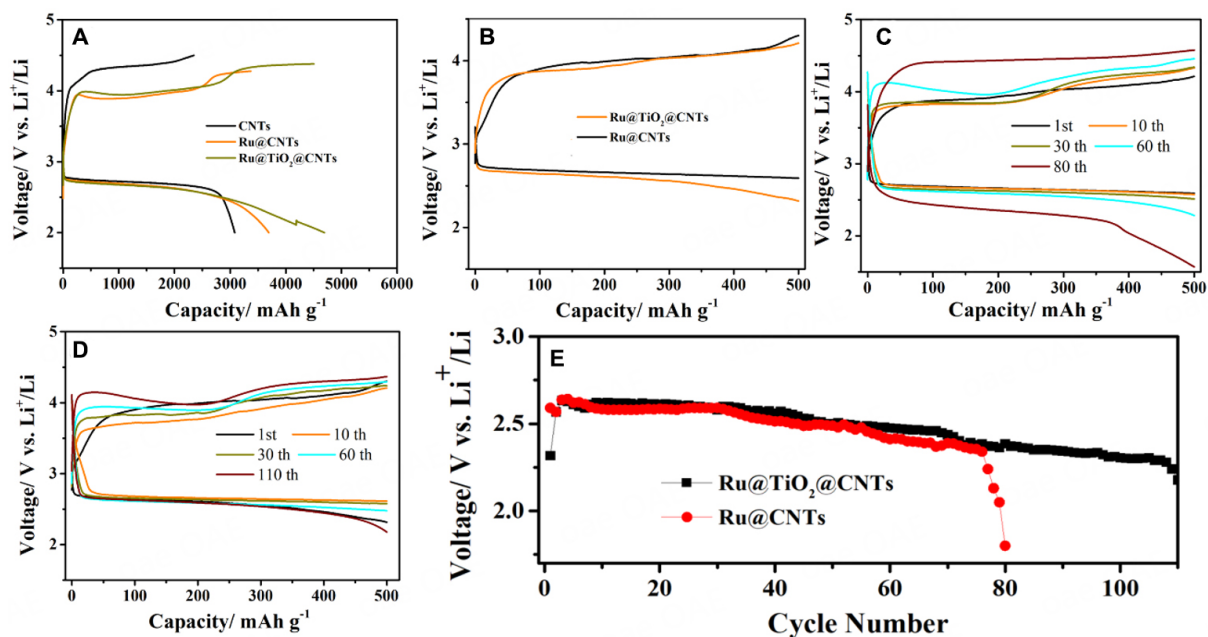


Figure 4. (A) Initial discharge and charge profiles of cells with different cathodes; (B) Initial discharge-charge plots of cells with different cathodes with a capacity limitation of 500 mAh g⁻¹ at a current density of 0.1 mA g⁻¹; Selected discharge-charge curves at different cycles of (C) Ru/CNTs and (D) Ru/TiO₂/CNTs (E) Potential-time curves of cells based on different cathodes at a current density of 100 mA g⁻¹ with a fixed specific capacity of 500 mAh g⁻¹.

cycles, the surface of the cathode was covered by tough solid materials and could be caused by the long-term degradation of the catalyst and side products [Figure 5F], which also predicted the end of the battery life. As is known, this is the fate of all the Li-O₂ batteries until the problems, e.g., electrolyte volatilization/

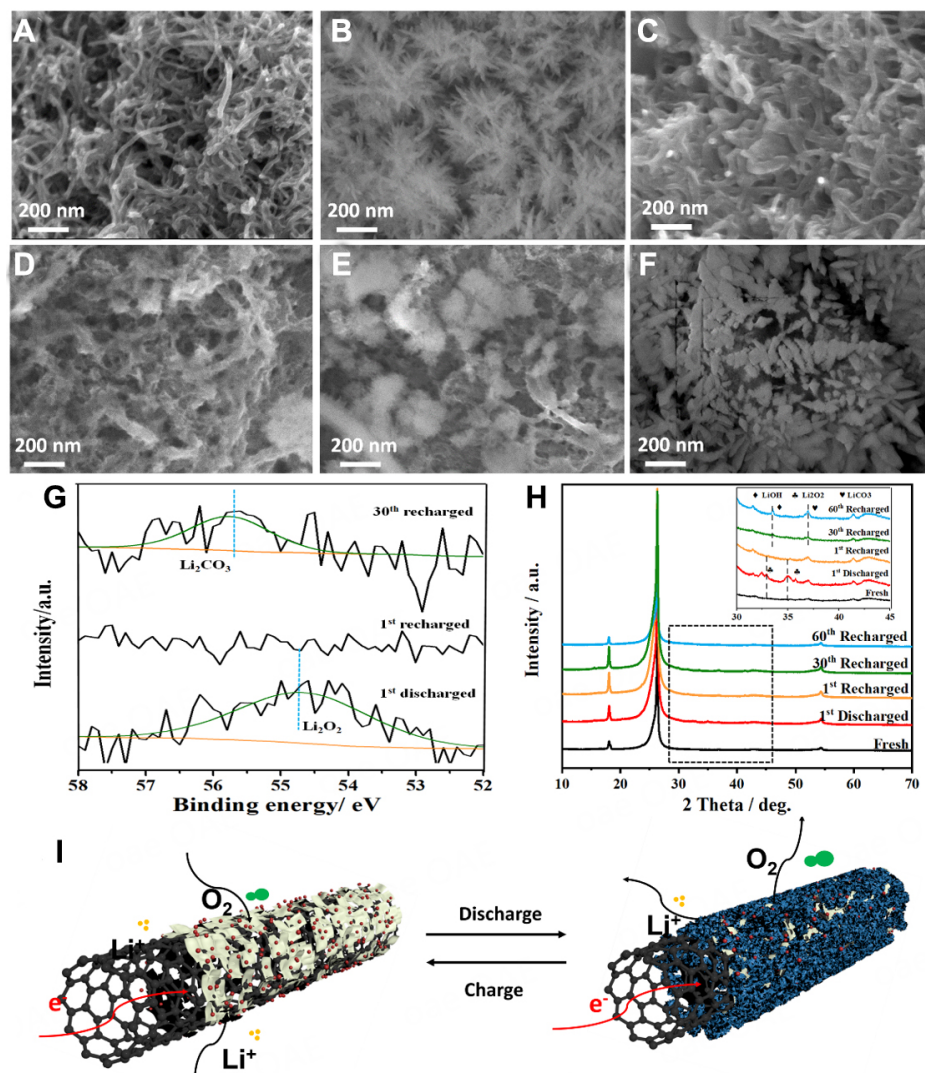


Figure 5. SEM images of the Ru/TiO₂/CNTs at different discharge stages: (A) fresh; (B) after first discharge; (C) after first recharge; (D) after 30 cycles; (E) after 60 cycles; (F) after 100 cycles; (G) High-resolution XPS spectra of Li 1s of Ru/TiO₂/CNTs after first discharged, recharge and 30 cycles; (H) XRD patterns of the Ru/TiO₂/CNTs cathode at different discharge/charge stages; (I) Schematic illustration of the feature structure of the Ru/TiO₂/CNTs after Li₂O₂ formation.

decomposition and carbon oxidation caused by the unique system, can be well solved. The XPS result showed a strong obvious Li 1s peak at 54.68 eV ascribing Li₂O₂ after the first discharge and the peak disappeared after recharge [Figure 5G], demonstrating that the as-prepared Ru/TiO₂/CNTs material could function as a bifunctional catalyst for Li-O₂ battery. One should note that there was no Li₂O₂ signal except a poor peak at 55.52 eV assigning to Li₂CO₃ appeared on the XPS spectra after 30 cycles. XRD measurements on the cathode at different cycling states were also conducted [Figure 5H]. It showed that the primary discharge product was Li₂O₂ and the reaction was based on the formation and decomposition of Li₂O₂. The XRD pattern of the cathode after 30th charge showed overlapped diffraction peaks (36.9°) of Li₂CO₃ and TiO₂. Li₂CO₃ is rooted in the decomposition of the ether-based electrolyte and it would accumulate on the electrode surface. XRD pattern of the electrode after 60 cycles of charging showed the co-existence of LiOH and Li₂CO₃. The former might come from the reaction of Li₂O₂ and a trace amount of H₂O, while the latter came from the gradual accumulation of Li₂CO₃ [35-37]. A concise schematic diagram [Figure 5I] illustrated the

feature structure of the Ru/TiO₂/CNTs material during discharging-charging process. The CNTs skeleton offered multiple three-dimensional channels for the rapid transportation of oxygen, Li⁺ and electrons, while a thin-loose layer of TiO₂ effectively inhibited the carbon corrosion but still could let mass transfer. The ultrafine Ru nanoparticles served as catalytic active sites. Therefore, a long-life Li-O₂ battery was constructed with the rational structure design of Ru/TiO₂/CNTs.

CONCLUSION

To sum up, we designed a Ru/TiO₂/CNTs cathode and successfully obtained it via a hydrolysis reaction of the titanium butoxide on the surface of CNTs, followed by aqueous reduction to load Ru. The as-prepared cathode combined consideration of the favorable kinetics of Li₂O₂-related main reaction and the avoidance of the side reaction caused by carbon cathode. Electrochemical results evidenced that the Ru/TiO₂/CNTs cathode could catalyze snow-like Li₂O₂-formation and more importantly the cathode still featured a porous state after discharge, which suggested quite friendliness on the subsequent charge and cycling process. As a result, the battery with Ru/TiO₂/CNTs cathode delivered a discharge capacity of about 4500 mAh g⁻¹ and a long lifespan of 110 at a current density of 100 mA g⁻¹. The concept of this research is of high value in directing the reasonable design of cathode material for Li-O₂ batteries.

DECLARATIONS

Authors' contributions

Conceived the manuscript: Liu L, Wu Y

Wrote the manuscript: Liu L, Zhou C, Fang W

Reviewed the manuscript: Liu L, Fang W, Wu Y

The discussion of the manuscript: Liu L, Zhou C, Fang W, Hou Y, Wu Y

Availability of data and materials

Not applicable.

Financial support and sponsorship

This work was supported by the Key R&D Program of the Ministry of Science and Technology (No. 2021YFB2400201), the National Natural Science Foundation of China (No. 52002171, 22101133, 22279055), the Natural Science Foundation of Jiangsu Province (No. BK20200696, No. BK20200768, No.20KJB430019).

Conflicts of interest

All authors declared that there are no conflicts of interest.

Ethical approval and consent to participate

Not applicable.

Consent for publication

Not applicable.

Copyright

© The Author(s) 2023.

REFERENCES

1. Kwak WJ, Rosy, Sharon D, et al. Lithium-oxygen batteries and related systems: potential, status, and future. *Chem Rev* 2020;120:6626-83. DOI PubMed
2. Lin D, Liu Y, Cui Y. Reviving the lithium metal anode for high-energy batteries. *Nat Nanotechnol* 2017;12:194-206. DOI PubMed

3. Johnson L, Li C, Liu Z, et al. The role of LiO₂ solubility in O₂ reduction in aprotic solvents and its consequences for Li-O₂ batteries. *Nat Chem* 2014;6:1091-9. DOI PubMed
4. Lyu Z, Zhou Y, Dai W, et al. Recent advances in understanding of the mechanism and control of Li₂O₂ formation in aprotic Li-O₂ batteries. *Chem Soc Rev* 2017;46:6046-72. DOI
5. Chi X, Li M, Di J, et al. A highly stable and flexible zeolite electrolyte solid-state Li-air battery. *Nature* 2021;592:551-7. DOI PubMed
6. Aurbach D, McCloskey BD, Nazar LF, Bruce PG. Advances in understanding mechanisms underpinning lithium-air batteries. *Nat Energy* 2016;1:1-11. DOI
7. Lim HD, Lee B, Bae Y, et al. Reaction chemistry in rechargeable Li-O₂ batteries. *Chem Soc Rev* 2017;46:2873-88. DOI
8. Lau S, Archer LA. Nucleation and growth of lithium peroxide in the Li-O₂ battery. *Nano Lett* 2015;15:5995-6002. DOI PubMed
9. Liu L, Liu Y, Wang C, et al. Li₂O₂ formation electrochemistry and its influence on oxygen reduction/evolution reaction kinetics in aprotic Li-O₂ batteries. *Small Methods* 2022;6:e2101280. DOI
10. Matsuda S, Yasukawa E, Kameda T, et al. Carbon-black-based self-standing porous electrode for 500 Wh/kg rechargeable lithium-oxygen batteries. *Cell Rep Phys Sci* 2021;2:100506. DOI
11. Zhao S, Zhang L, Zhang G, Sun H, Yang J, Lu S. Failure analysis of pouch-type Li-O₂ batteries with superior energy density. *J Energy Chem* 2020;45:74-82. DOI
12. Dou Y, Wang X, Wang D, et al. Tuning the structure and morphology of Li₂O₂ by controlling the crystallinity of catalysts for Li-O₂ batteries. *Chem Eng J* 2021;409:128145. DOI
13. Song LN, Zhang W, Wang Y, et al. Tuning lithium-peroxide formation and decomposition routes with single-atom catalysts for lithium-oxygen batteries. *Nat Commun* 2020;11:2191. DOI PubMed PMC
14. Liu Y, Wang K, Peng X, et al. Formation/decomposition of Li₂O₂ induced by porous NiCeO_x nanorod catalysts in aprotic lithium-oxygen batteries. *ACS Appl Mater Interfaces* 2022;14:16214-21. DOI PubMed
15. Chen C, Xu S, Kuang Y, et al. Nature-inspired tri-pathway design enabling high-performance flexible Li-O₂ batteries. *Adv Energy Mater* 2019;9:1802964. DOI
16. Lin X, Yuan R, Cai S, et al. An open-structured matrix as oxygen cathode with high catalytic activity and large Li₂O₂ accommodations for lithium-oxygen batteries. *Adv Energy Mater* 2018;8:1800089. DOI
17. Huang Z, Deng Z, Shen Y, et al. A Li-O₂ battery cathode with vertical mass/charge transfer pathways. *J Mater Chem A* 2019;7:3000-5. DOI
18. Liu L, Ma T, Fang W, et al. Facile fabrication of Ag nanocrystals encapsulated in nitrogen-doped fibrous carbon as an efficient catalyst for lithium oxygen batteries. *Energy Environ Mater* 2021;4:239-45. DOI
19. Peng X, Wang C, Liu Y, et al. Critical advances in re-engineering the cathode-electrolyte interface in alkali metal-oxygen batteries. *Energy Mater* 2022;1:100011. DOI
20. Tan P, Jiang H, Zhu X, et al. Advances and challenges in lithium-air batteries. *Appl Energy* 2017;204:780-806. DOI
21. Thotiyl MM, Freunberger SA, Peng Z, Bruce PG. The carbon electrode in nonaqueous Li-O₂ cells. *J Am Chem Soc* 2013;135:494-500. DOI
22. Jung J, Cho S, Nam JS, Kim I. Current and future cathode materials for non-aqueous Li-air (O₂) battery technology - a focused review. *Energy Stor Mater* 2020;24:512-28. DOI
23. Liu L, Guo H, Fu L, et al. Critical advances in ambient air operation of nonaqueous rechargeable Li-air batteries. *Small* 2021;17:e1903854. DOI PubMed
24. Liu L, Hou Y, Wang J, et al. Nanofibrous Co₃O₄/PPY hybrid with synergistic effect as bifunctional catalyst for lithium-oxygen batteries. *Adv Mater Interfaces* 2016;3:1600030. DOI
25. Chen Y, Freunberger SA, Peng Z, Fontaine O, Bruce PG. Charging a Li-O₂ battery using a redox mediator. *Nat Chem* 2013;5:489-94. DOI PubMed
26. Lim HD, Song H, Kim J, et al. Superior rechargeability and efficiency of lithium-oxygen batteries: hierarchical air electrode architecture combined with a soluble catalyst. *Angew Chem Int Ed* 2014;53:3926-31. DOI PubMed
27. Zhang L, Zhang D, Zhang J, et al. Design of meso-TiO₂@MnO_x-CeO_x/CNTs with a core-shell structure as DeNO_x catalysts: promotion of activity, stability and SO₂-tolerance. *Nanoscale* 2013;5:9821-9. DOI PubMed
28. Demir E, Akbayrak S, Önal AM, Özkaz S. Nanoceria-supported ruthenium(0) nanoparticles: highly active and stable catalysts for hydrogen evolution from water. *ACS Appl Mater Interfaces* 2018;10:6299-308. DOI PubMed
29. Sa YJ, Kwon K, Cheon JY, Kleitz F, Joo SH. Ordered mesoporous Co₃O₄ spinels as stable, bifunctional, noble metal-free oxygen electrocatalysts. *J Mater Chem A* 2013;1:9992-10001. DOI
30. Dong Y, He K, Yin L, Zhang A. A facile route to controlled synthesis of Co₃O₄ nanoparticles and their environmental catalytic properties. *Nanotechnology* 2007;18:435602. DOI
31. Liu X, Zhao L, Xu H, et al. Tunable cationic vacancies of cobalt oxides for efficient electrocatalysis in Li-O₂ batteries. *Adv Energy Mater* 2020;10:2001415. DOI
32. Gopiraman M, Karvembu R, Kim IS. Highly active, selective, and reusable RuO₂/SWCNT Catalyst for heck olefination of aryl halides. *ACS Catal* 2014;4:2118-29. DOI
33. Kim Y, Park JH, Kim JG, et al. Ruthenium oxide incorporated one-dimensional cobalt oxide composite nanowires as lithium-oxygen battery cathode catalysts. *ChemCatChem* 2017;9:3554-62. DOI

34. Xu JJ, Chang ZW, Wang Y, Liu DP, Zhang Y, Zhang XB. Cathode surface-induced, solvation-mediated, micrometer-sized Li_2O_2 cycling for Li- O_2 batteries. *Adv Mater* 2016;28:9620-8. DOI
35. Thotiyl MM, Freunberger SA, Peng Z, Chen Y, Liu Z, Bruce PG. A stable cathode for the aprotic Li- O_2 battery. *Nat Mater* 2013;12:1050-6. DOI
36. Zhang P, Zhao Y, Zhang X. Functional and stability orientation synthesis of materials and structures in aprotic Li- O_2 batteries. *Chem Soc Rev* 2018;47:2921-3004. DOI
37. Balaish M, Jung J, Kim I, Ein-Eli Y. A critical review on functionalization of air-cathodes for nonaqueous Li- O_2 batteries. *Adv Funct Mater* 2020;30:1808303. DOI